JOURNAL OF VIROLOGY, Mar. 2002, p. 2848–2856 Vol. 76, No. 6
0022-538X/02/$04.00+0 DOI: 10.1128/JVI.76.6.2848–2856.2002
Copyright © 2002, American Society for Microbiology. All Rights Reserved.

Solution Structure of the Viral Receptor Domain of Tva and Its Implications in Viral Entry

Qing-Yin Wang,[1] Wen Huang,[2] Klavs Dolmer,[2] Peter G. W. Gettins,[2] and Lijun Rong[1]*

Department of Microbiology and Immunology[1] and Department of Biochemistry and Molecular Biology,[2] College of Medicine, University of Illinois at Chicago, Chicago, Illinois 60612

Received 14 September 2001/Accepted 7 December 2001

Tva is the cellular receptor for subgroup A avian sarcoma and leukosis virus (ASLV-A). The viral receptor function of Tva is determined by a 40-residue, cysteine-rich motif called the LDL-A module. Here we report the solution structure of the LDL-A module of Tva, determined by nuclear magnetic resonance (NMR) spectroscopy. Although the carboxyl terminus of the Tva LDL-A module has a structure similar to those of other reported LDL-A modules, the amino terminus adopts a different conformation. The LDL-A module of Tva does not contain the signature antiparallel β-sheet observed in other LDL-A modules, and it is more flexible than other reported LDL-A modules. The LDL-A structure of Tva provides mechanistic insights into how a simple viral receptor functions in retrovirus entry. The side chains of H38 and W48 of Tva, which have been identified as viral contact residues by mutational analysis, are solvent exposed, suggesting that they are directly involved in EnvA binding. However, the side chain of L34, another potential viral contact residue identified previously, is buried inside of the module and forms the hydrophobic core with other residues. Thus L34 likely stabilizes the Tva structure but is not a viral interaction determinant. In addition, we propose that the flexible amino-terminal region of Tva plays an important role in determining specificity in the Tva-EnvA interaction.

Infection by subgroup A avian sarcoma and leukosis virus (ASLV-A) is initiated by specific interactions between viral glycoprotein EnvA and its cognate receptor, Tva. Tva plays at least two important roles in this process. First, the high-affinity binding between EnvA and Tva allows specific attachment of ASLV-A virions to susceptible avian host cells (1, 11, 29, 40). Second, Tva binding is responsible for a series of conformational changes on EnvA (called Tva triggering), which appear to be essential for EnvA-mediated virus-host membrane fusion (5, 12, 15). Because receptor triggering is a common, yet poorly understood, mechanism for entry of various enveloped viruses, analysis of ASLV-A infection serves as an excellent model in elucidating the basic principles in retrovirus entry.

Tva is a small membrane-associated glycoprotein (2). All evidence suggests that Tva is the only receptor required for ASLV-A entry. Within the extracellular domain of Tva is a 40-residue motif, called an LDL-A module, which is highly homologous to the human low-density lipoprotein receptor (LDLR) ligand-binding repeats (LDL-A modules). It has been demonstrated that the LDL-A module of Tva is necessary and sufficient to mediate efficient EnvA binding and ASLV-A infection (26). Furthermore, this module of Tva can be functionally replaced by the fourth repeat of human LDLR with minor amino acid substitutions (28). These results indicate that an individual LDL-A module can independently mediate protein-protein interaction. We have shown recently that calcium is required for proper folding of the Tva LDL-A module in vitro (34), suggesting that the folding of this module is similar to that of other LDL-A modules.

* Corresponding author. Mailing address: Department of Microbiology and Immunology, College of Medicine, University of Illinois at Chicago, E829 MSB, 835 S. Wolcott Ave., Chicago, IL 60612. Phone: (312) 355-0203. Fax: (312) 996-6415. E-mail: lijun@uic.edu.

The human LDLR is the prototype of the LDLR superfamily, which also includes the very-low-density lipoprotein receptor, and the LDLR-related protein (LRP). All members of the LDLR family contain at least one LDL-A module, which is believed to mediate extracellular protein-protein interactions. Each module is roughly 40 amino acids in length and includes six invariable cysteines and several highly conserved acidic residues. Structures of six individual LDL-A modules have been determined by NMR spectroscopy or X-ray crystallography (3, 4, 6, 10, 18, 25). These structures gave insightful information on LDLR folding and function. All of these modules adopt highly similar three-dimensional conformations, which consist of a short antiparallel β-sheet and a one-turn α-helix. The structure is stabilized by three pairs of disulfide bonds formed by the invariable cysteines. Furthermore, six residues, including four highly conserved acidic residues at the carboxyl terminus of the module, are involved in calcium coordination.

In this study, we determined the solution structure of the LDL-A module of Tva by nuclear magnetic resonance (NMR) spectroscopy. We show that the Tva module does not contain the signature antiparallel β-sheet in the N-terminal region observed in other LDL-A modules and that the backbone in this region is more mobile than elsewhere in the domain, suggesting that its N terminus is more flexible. Thus, the Tva LDL-A module defines a novel three-dimensional conformation for LDL-A modules. The flexible N-terminal structure of the Tva module may change its conformation upon EnvA binding to promote high-affinity binding between Tva and EnvA. Furthermore, the structure explains the roles of the putative viral interaction determinants of Tva, which have been previously identified by mutational analysis, in protein folding and in mediating ASLV-A entry. The side chains of H38 and W48 are solvent exposed, strongly suggesting that these residues are directly involved in an interaction with EnvA. However, L34 is

Downloaded from http://jvi.asm.org/ on October 28, 2020 by guest

most likely responsible for protein folding and the structure stability of Tva. Therefore, this structure provides a molecular basis for us to elucidate the basic principles in retrovirus entry.

MATERIALS AND METHODS

Cloning and preparation of the Tva LDL-A module. The quail Tva LDL-A module (2) was expressed as a glutathione *S*-transferase (GST) fusion protein as described previously (34). In brief, the ^{13}C- and ^{15}N-double-labeled or ^{15}N-labeled fusion protein was expressed in *Escherichia coli* in minimal medium containing 0.6% basal medium Eagle vitamin solution (Gibco), 1 g of $(^{15}NH_4)_2SO_4$, and 2 g of ^{13}C-labeled or unlabeled glucose. Protein expression was induced by IPTG (isopropyl-β-D-thiogalactopyranoside) and purified as described previously (34). The GST portion was removed by thrombin cleavage. In vitro refolding and purification of the Tva LDL-A module were performed as described by Wang et al. (34). The lyophilized Tva LDL-A module was dissolved in 20 mM CH_3COOH–10 mM $CaCl_2$-10% D_2O, pH 5.3. The final protein concentration of the module was 2 mM.

NMR spectroscopy. All NMR spectra were recorded at the University of Illinois at Chicago on a Bruker DRX600 equipped with a pulsed-field gradient accessory and operating at 600.13 MHz for ^{1}H. Center frequencies were 4.70 parts per million for ^{1}H, 118 ppm for ^{15}N, 55 ppm for $^{13}C_\alpha$, and 43 ppm for $^{13}C_{\alpha\beta}$. Initially, attempts to record spectra at 298°K were made, but only a few nuclear Overhauser effect (NOE) cross-peaks were detected during the acquisition of NOE spectroscopy (NOESY) experiments at this temperature. Therefore, several two-dimensional NOESY experiments were performed to determine the optimal temperature for spectral acquisition. Numerous well-defined cross-peaks were detected at 282°K. Thus all spectral acquisition was conducted at 282°K for the structure determination. NMR raw data were processed and analyzed using Triad, version 6.3, software (Tripos, Inc.). Backbone sequential assignment was obtained by triple-resonance experiments HNCA (13) and HNCACB (36). ^{15}N-edited total-correlation spectroscopy (TOCSY)-heteronuclear single quantum correlation spectroscopy (HSQC) experiments (38) were carried out to assign most of the side chain protons. The ambiguities in α- and β-proton assignment (e.g., threonine and serine) were resolved by their attached carbon in an HCCH-TOCSY experiment (19). A two-dimensional NOESY experiment and two three-dimensional NOESY experiments including a ^{15}N-edited NOESY-HSQC (32) and a ^{1}H-^{13}C-correlated HCCH-NOESY (24) were performed to acquire NOE information; the mixing time was 300 ms. Two-dimensional NOESY was recorded using an unlabeled protein sample dissolved in D_2O buffer. ^{13}C-HCCH-NOESY was recorded in D_2O. Torsion angle constraints were obtained from an HNHA experiment (33). Evidence for hydrogen bonds was derived from solvent exchange of amide protons, in which the lyophilized ^{15}N-labeled Tva LDL-A module protein was freshly dissolved in a buffer containing 99% D_2O just before acquisition of a series of [^{1}H-^{15}N]-HSQC spectra, each of which was recorded for 30 min.

Backbone dynamics of the Tva LDL-A module and of CR8 were examined by measuring ^{15}N T_1 and T_2 relaxation times and ^{1}H-^{15}N NOEs. All spectra were recorded at 298°K using the pulse sequences published previously (9). Longitudinal relaxation (T_1) parameters were determined from spectra recorded with seven T delays of 10, 120, 240, 360, 470, 580, and 700 ms. Transverse relaxation (T_2) experiments were performed with seven T delays of 8, 48, 104, 168, 216, 256, and 304 ms. The ^{1}H-^{15}N NOE experiments were carried out in the presence or absence of a 3-s proton presaturation period.

Resonance assignments. The recombinant Tva LDL-A module protein contains 47 amino acids including the 40-residue LDL-A module, four additional residues (GSSR) at the N terminus, and three (GTS) at the C terminus, which are derived from the expression vector (34). The [^{1}H-^{15}N]-HSQC spectrum of the protein displayed a good dispersion of chemical shifts in the presence of calcium. Individual amino acids were initially identified and determined from their C_α, C_β, H_α, and H_β chemical shifts by sequential assignment, that is, by matching intra- and interresidue $^{13}C_\alpha$ and/or $^{13}C_\beta$ chemical shifts for a given residue (characteristic residues such as glycine or alanine were used) to its previous residue in the protein sequence. Small sequence segments (e.g., Gly-Thr-Ser at the C terminus and Pro-Gly pairs) were thus assigned by using this method. These small sequence segments were subsequently assigned to regions in the protein. Most of the side chain proton assignments were acquired from ^{15}N-edited TOCSY-HSQC and ^{13}C-edited HCCH-TOCSY experiments.

Constraints and structure calculation. For each NOESY experiment, NOESY peaks were picked and identified according to the chemical shift assignments. These NOE constraints were further ranked into strong, medium, and weak on the basis of cross-peak intensities. Upper distance limits of 3.0, 4.0, and 5.0 Å between backbone atoms, of 3.5, 4.5, and 5.5 Å between backbone-side chain atoms, and of 6.0 Å between side chain-side chain atoms were placed. The dihedral angle ϕ constraints were derived from $J(H^NN^\alpha)$ coupling constants measured by an HNHA experiment (33). Conversion of J values into the torsion angle constraints was solved by a Karplus equation. Dihedral angle ψ was not constrained during the structure calculation.

Structure calculation for the Ca^{2+}-Tva LDL-A module was performed by using DYANA (14), a torsion angle dynamics annealing simulation program. The input data for calculation included the distance constraints (NOEs for backbone-backbone, backbone-side chain, and side chain-side chain), ϕ torsion angle constraints, and two hydrogen bonds derived from a proton exchange HSQC experiment. Three disulfide bonds and calcium coordination were used as additional constraints before simulated annealing. The disulfide connectivity of the Tva LDL-A module was based on the sequence alignment of all the LDL-A modules. The 20 calculated structures with the lowest target function were used for analysis of constraint violation and for further assignment of NOEs for the subsequent rounds. This step was repeated until all of the NOE peaks were assigned, all the dihedral angle constraints were added, and there was no distance violation greater than 0.31 Å. During the final step, 200 initial structures were calculated, from which 20 structures with the lowest target function were picked for the final structure. A structure comparison between the Tva LDL-A module and CR8 and a three-dimensional structure display were made with MOLMOL (20).

Analysis of relaxation parameters. All NMR data were processed using Triad, version 6.3, software (Tripos, Inc.). The $R1$ ($1/T1$) and $R2$ ($1/T2$) relaxation rates were determined by nonlinear fits of the measured peak heights to two-parameter function $I(t) = I_0\exp(-tR_i)$. The ^{1}H-^{15}N NOE enhancements were calculated from the ratio of the intensities of peaks in the spectra acquired in the presence or absence of proton saturation, $NOE = I_{sat}/I_{unsat}$. The standard deviation of the NOEs was derived from the background noise as described by Farrow et al. (9).

NMR relaxation parameters $R1$ and $R2$ and the NOEs were used as input data for a model-free analysis of internal mobility by the program TENSOR 2 (8), which uses a Lipari-Szabo type analysis: $J(\omega) = S_2^2\{[S_1^2\tau_c/(1 + \omega^2\tau_c^2)] + [(1 - S_1^2)\tau'/(1 + \omega^2\tau'^2]\}$ where $\tau' = \tau_c\tau_i/(\tau_c + \tau_i)$. For CR8, model 1 was used for residues 14, 17, 19, 26, 27, 32, 33, and 41; model 4 was used for residues 1, 2, 10, 11, 15, 16, 29, and 37; model 5 was used for residues 4, 30, 42, and 44; and the rest of the residues were fitted to model 2. For the Tva LDL-A module, model 2 was used for residues −2, 15, 27, 47, 49, 50, and +3; model 3 was used for residues 33, 34, 35, 40, and 43; model 4 was used for residues 18, 23, 38, and 45; model 5 was used for residues −1, 24, +1, and +2; and the rest of the residues were fitted to model 1. For the nomenclature of the plus and minus signs, see the legend for Fig. 5.

Accession number. The structure of the Tva LDL-A module described in this paper has been deposited in the Protein Data Bank with accession number 1JRF.

RESULTS AND DISCUSSION

Structure determination. A uniformly ^{13}C- and ^{15}N-double-labeled or ^{15}N-labeled quail Tva LDL-A module was expressed as a GST fusion protein in *E. coli*. After thrombin cleavage, the module was refolded and purified as described previously (34). Since calcium is necessary for the correct folding and structure integrity of the Tva LDL-A module, all NMR spectra were acquired in the presence of a saturating level of calcium (10 mM). The spectra were recorded at 600 MHz at temperatures of 298 and 282°K. However, since only a few cross-peaks could be identified in the three-dimensional NOESY spectra at 298°K due to the structure flexibility of the Tva LDL-A module, assignment and structure calculations were performed based on the spectra recorded at 282°K. At this temperature, the HSQC spectrum of the Tva LDL-A module protein gave a good dispersion and only minor chemical shift differences relative to spectra obtained at 298°K were observed (≤0.3 ppm for ^{1}H-NH and ≤0.4 ppm for ^{15}N-NH; data not shown). These results suggest that this protein maintains similar structures at 282 and 298°K. Although the Ca^{2+}-bound module displayed good spectral dispersion in the HSQC spectrum, two sets of

Downloaded from http://jvi.asm.org/ on October 28, 2020 by guest

TABLE 1. Constraints used in structure determination

Constraint	No.
NOE constraints	
Intraresidue	133
Sequential ($\|i - j\| = 1$)	119
Medium range ($1 < \|i - j\| < 5$)	38
Long range ($\|i - j\| \geq 5$)	53
Torsion angle constraints	29
Disulfide bonds	3
Hydrogen bonds	2

resonance (relative ratio, 70:30) could be identified for residues in the amino terminus, G14, E20, G23, A24, H25, G26, and E27 (data not shown), both at high (~2 mM) and low (~100 μM) protein concentrations. This most likely resulted from *cis-trans* isomerization of prolines (P12, P13, P21, and P22) in that region (37). For example, NOE cross-peaks between the amide proton and the α-proton of E20 and the δ-proton of P21 for the major conformer (70%) were detected, suggesting a *trans*-P21 peptide bond, while, for the minor conformer (30%), NOE cross-peaks between the α-proton of E20 and the α-proton of P21 were observed, suggesting a *cis*-P21 peptide bond. The solution structure of the Tva LDL-A module reported here represents the major conformer. The chemical shift assignments were obtained from the following experiments: [^{1}H-^{15}N]-HSQC, HNCA, and HNCACB experiments for assigning the backbone atoms and C_β and ^{15}N-edited TOCSY-HSQC and ^{13}C-edited HCCH-TOCSY experiments for assigning the side chain protons.

A two-dimensional NOESY experiment and two three-dimensional NOESY experiments (^{15}N-edited NOESY-HSQC and ^{1}H-^{13}C-correlated HCCH-NOESY experiments) were performed to obtain NOE information. An HNHA experiment was carried out for measuring $J(H^N N^\alpha)$ coupling constants, which were converted to dihedral angle ϕ by using the Karplus equation. A total of 29 ϕ angle constraints were used. Eight slowly exchanging amide protons were identified from an exchange experiment, among which backbone amides of residues W33 and L34 were associated with the one-turn α-helix and the remaining six were either calcium-binding residues (D36 and E47) or those near the calcium-binding region (C35, G37, R45, and W48).

A set of 200 initial structures was generated by torsion angle dynamics annealing simulation program DYANA (14). A total of 343 NOE upper distance constraints, 29 torsion angle constraints, 3 disulfide bonds based on sequence alignment, and 2 hydrogen bonds (in the α-helix) were used as input data for the calculation (Table 1). The 20 best structures (Fig. 1) with the lowest target function were selected, none of which had a distance constraint violation greater than 0.31 Å. The root mean square deviations (RMSD) from the mean structure for the backbone are 0.61 (from the first to the sixth cysteine), 0.48 (from the first to the third cysteine), and 0.45 Å (from the third to the sixth cysteine), respectively (Table 2).

TABLE 2. Structure statistics for the 20 best structures shown in Fig. 1

Residue	RMSD (Å) to mean structure[a]	Pairwise RMSD (Å)
Backbone (47[b])	1.85 ± 0.53	1.90 ± 0.52
Backbone (11–50, C1–C6)	0.61 ± 0.21	0.63 ± 0.21
Backbone (11–28, C1–C3)	0.48 ± 0.25	0.50 ± 0.26
Backbone (28–50, C3–C6)	0.45 ± 0.12	0.47 ± 0.12
Heavy atom (47[b])	2.17 ± 0.45	2.24 ± 0.42
Heavy atom (11–50, C1–C6)	1.27 ± 0.21	1.30 ± 0.18
Heavy atom (11–28, C1–C3)	1.04 ± 0.21	1.07 ± 0.19
Heavy atom (28–50, C3–C6)	1.26 ± 0.22	1.30 ± 0.20

[a] RMSD was calculated by using MOLMOL.
[b] The recombinant Tva LDL-A module contains 47 amino acids including four additional residues at the N terminus and three at the C terminus.

Structure of the Tva LDL-A module. The structure of the Tva LDL-A module is shown in Fig. 2A. It consists of two loops, which are connected by a one-turn α-helix at the bottom and a disulfide bond between the second and the fifth invariable cysteines at the top. The N-terminal loop (from the first to the third cysteine) is held together by a disulfide bond between the first and the third cysteines. It also contains a small hydrophobic core formed by F16, P21, and L34 (see Fig. 6), since NOE cross-peaks were observed in the two-dimensional NOESY spectrum among these residues (data not shown). This hydrophobic core contributes to the structural stability. Surprisingly, there is no recognizable antiparallel β-sheet in this region, as found in other LDL-A modules. Additionally, the β-turn structure, formed by residues H7 to E10 in CR8 (18), is also absent in this module. The only identifiable secondary structure is a one-and-one-fourth-turn α-helix, which is formed by residues P30, Q31, D32, W33, and L34. The evidence to support this was derived from the following observations. NOE cross-peaks were detected in the ^{15}N-NOESY-

FIG. 1. Stereo view of the 20 selected structures of the Tva LDL-A module with the lowest target function from the final DYANA calculations.

Downloaded from http://jvi.asm.org/ on October 28, 2020 by guest

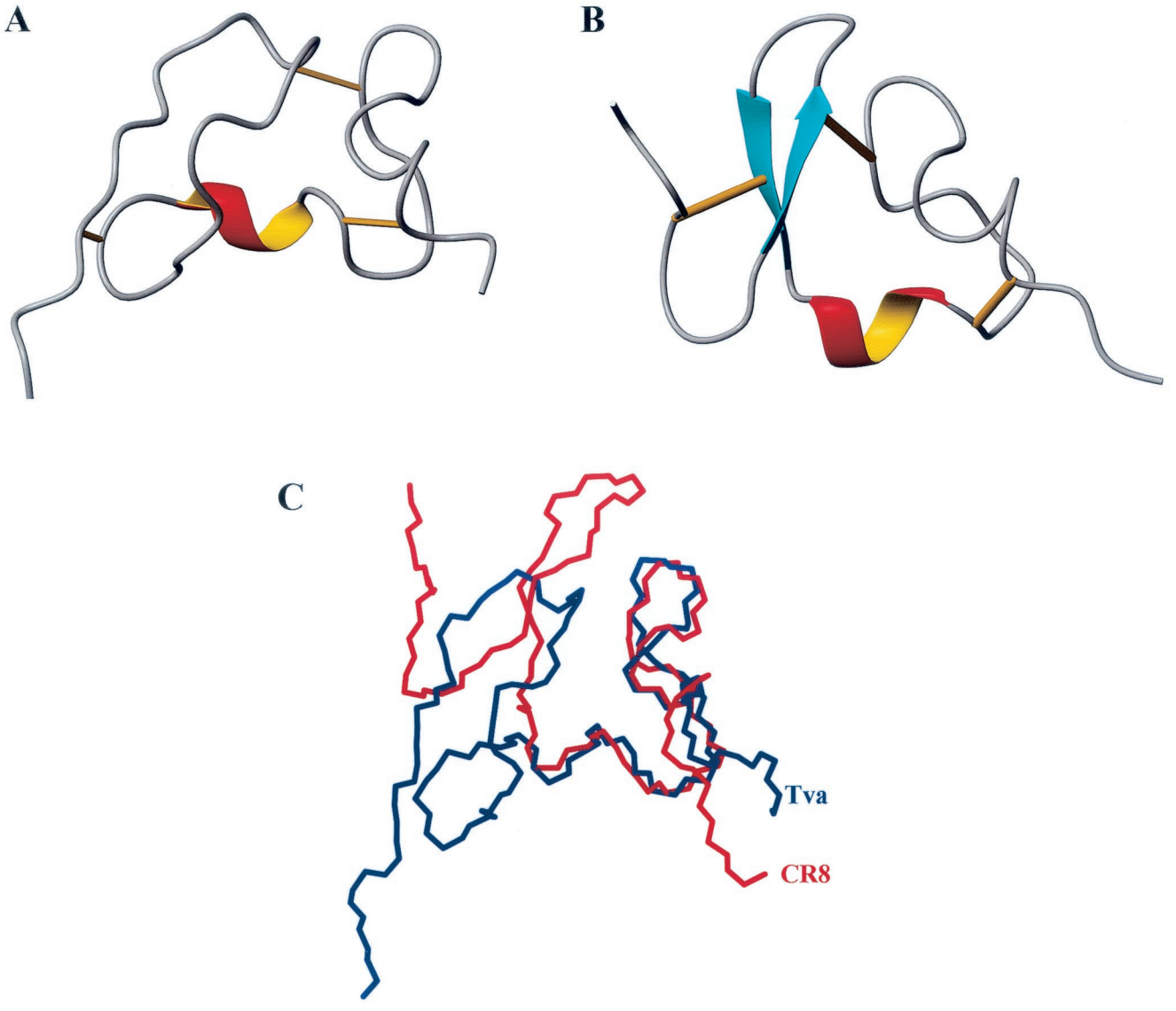

FIG. 2. Structure comparison of the Tva LDL-A module and LRP CR8. Left, N terminus; right, C terminus. Cyan, β-sheet; red and yellow, α-helix. Bottom right, calcium-binding site; straight lines, three disulfide bonds. (A) Ribbon representation of the final structure of the Tva LDL-A module, based on the 20 best structures shown in Fig. 1. (B) Ribbon representation of the three-dimensional solution structure of CR8. (C) Superimposition of the backbone of the Tva LDL-A module (blue) and that of CR8 (red).

HSQC spectrum between the α-proton of P30 and the amide proton of W33 and between the α-proton of Q31 and the amide proton of L34. In addition, the proton exchange experiment showed that the backbone amides of W33 and L34 were protected against hydrogen exchange. These results indicate that the α-helix is stabilized by two hydrogen bonds formed between W33 and P30 and between L34 and Q31. This short α-helix bridges the N-terminal and C-terminal loops. The absence of well-defined secondary structures suggests conformational flexibility of this module, especially in the N-terminal region. The C-terminal loop (from the third to the sixth cysteine) is held together by a disulfide bond between the fourth and the sixth cysteines. The LDL-A module of Tva, like all other LDL-A modules, contains a calcium binding site, where calcium serves as a bridge connecting the front and the back parts of the loop (Fig. 3A).

Six individual LDL-A module structures have been determined previously either by NMR spectroscopy or by X-ray crystallography (3, 4, 6, 10, 18, 25). All of them adopt very similar three-dimensional conformations, including three pairs of disulfide bonds, a Ca^{2+} cage, a one-turn α-helix, and an antiparallel β-sheet. Shown in Fig. 2B is the solution structure of LRP CR8 (18), and shown in Fig. 2C is a superpositioning of CR8's backbone with that of the Tva LDL-A module for comparison. The C-terminal loop of the Tva LDL-A module adopts an overall conformation similar to those of other LDL-A modules and contains a one-turn α-helix, and a calcium cage. Comparison of the backbones of Tva and CR8 shows only minor variation (RMSD, 1.14 Å) for the calcium-binding loop (residues 33 to 50). The structure is stabilized by three pairs of disulfide bonds. However, the N-terminal loop of the Tva module displays interesting and novel features. It does

Downloaded from http://jvi.asm.org/ on October 28, 2020 by guest

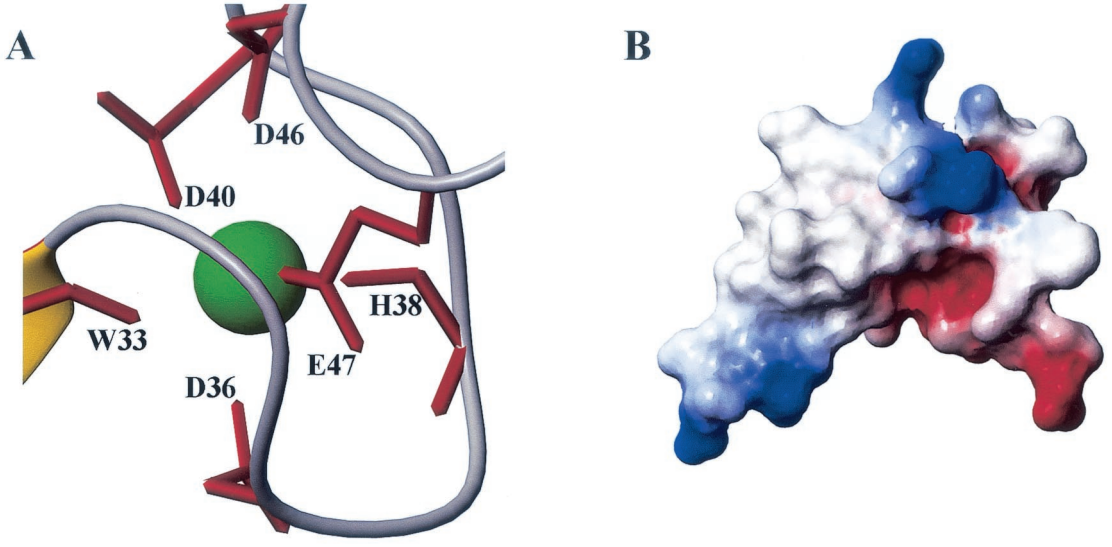

FIG. 3. (A) Calcium-coordinating site of the Tva LDL-A module. (B) Electrostatic surface of the Tva LDL-A module. The structure is in the same orientation as the structure in Fig. 2A; red, negative charge; blue, positive charge.

not contain the signature antiparallel β-sheet observed in other LDL-A modules. Therefore, this structure represents a new class of LDL-A module conformation.

We propose that D36, D40, D46, and E47 (via their side chains) and W33 and H38 (via their carbonyl oxygens) form the calcium cage in the Tva LDL-A module (Fig. 3A). Previously we demonstrated that correct folding of the Tva LDL-A module is Ca^{2+} dependent just like that of other LDL-A modules. Thus calcium coordination of the Tva LDL-A module is modeled on the X-ray crystal structure of human LDL-A5 and is supported by our experimental data. It is expected that mutations of the calcium-binding acidic residues would disrupt the correct folding of the module even in the presence of calcium. Indeed, the D46A and E47A mutant proteins were shown to be incorrectly folded (34), strongly supporting the role of these two residues in calcium coordination. The involvement of W33 in calcium binding was demonstrated by the ^{15}N chemical shift of the amide of L34. The amide nitrogen of L34 was downfield shifted about 4 ppm compared to the random coil value (observed value of 125.9 ppm relative to a random coil value of 121.8 ppm [35]). Although the roles of D36, D40, and H38 in calcium binding are based on sequence alignment, we are confident that these residues are involved in calcium binding. Recently, the X-ray crystal structure of LRP CR7 was determined, and it was found that residues of CR7 corresponding to D36, D40, and H38 of Tva, like those of human LDL-A5, are involved in calcium coordination (M. Simonovic, K. Dolmer, W. Huang, D. K. Strickland, K. Volz, and P. G. W. Gettins, submitted for publication). Inspection of the electrostatic surface of the Tva LDL-A module shows that the surface of the calcium-binding region is negatively charged (Fig. 3B), which is also true for other LDL-A modules with known structures. However, the role of this negatively charged surface in ligand binding is not clear.

Structural analysis of the Tva LDL-A module by protein secondary structure prediction (30) suggests that this module contains the signature antiparallel β-sheet in the N terminus. However, as discussed above, one major difference between the Tva LDL-A module and others is the absence of this antiparallel β-sheet in Tva. This conclusion is supported by the experimental data. The α-proton chemical shifts of several LRP CR8 residues which are involved in the formation of the antiparallel β-sheet (18) were significantly downfield shift. In contrast, a downfield shift in the corresponding region of the Tva module was not detected (data not shown), suggesting that this region of Tva does not form the β-sheet (35). In addition, it was found that the backbone amide of F16 of Tva is not involved in hydrogen bonding. F16 is conserved in all the LDL-A modules, and it was shown to be involved in hydrogen bonding to form the antiparallel β-sheet in other reported LDL-A structures. However, the solvent exchange experiment showed that the backbone amide of F16 was not protected, indicating that it was not involved in hydrogen bond formation in the Tva module. Closer examination of the LDL-A module of Tva by sequence alignment with other LDL-A modules shows that the N terminus of the Tva module (from the first to the third cysteine) is quite different from those of other LDL-A modules both in spacing and in sequence, while the C terminus (from the third to the sixth cysteine) is more similar (Fig. 4). In particular, there are nine residues between the second and the third cysteines for the Tva LDL-A module, whereas six LDL-A modules with known structures contain only four to six residues (Fig. 4). In retrospect, since residues within this region participate in the formation of the antiparallel β-sheet in other LDL-A modules, it is not surprising that the LDL-A module adopts a novel fold. The difference in LDL-A module conformation must reflect and dictate specificity in ligand interaction. As will be discussed below, the N terminus of the Tva LDL-A module plays a critical role in optimal viral receptor function.

One interesting question to be answered is whether the Tva LDL-A structure is really unique among the hundreds of LDL-A modules. Considering the diverse roles of these modules in biological processes, it is possible that some other LDL-A modules may adopt conformations similar to that of

Downloaded from http://jvi.asm.org/ on October 28, 2020 by guest

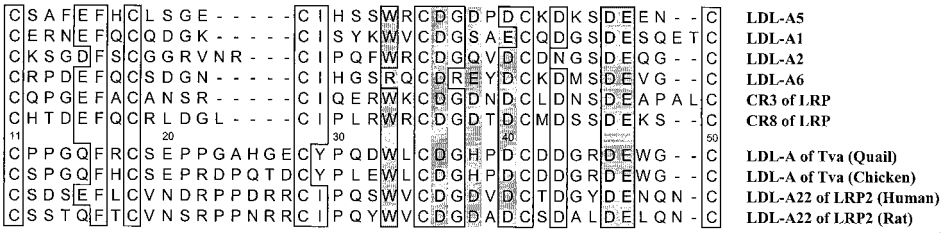

FIG. 4. Amino acid sequence alignment of the Tva LDL-A module, LDL-A22 of LRP2, and all LDL-A modules with known structures: LDL-A5, LDL-A1, LDL-A2, LDL-A6, LRP CR3, and CR8. Conserved amino acids are boxed, and the six residues involved in calcium coordination are shaded. The residues of the Tva LDL-A module from both quail and chickens are numbered from 11 to 50 according to the mature Tva (2).

the Tva LDL-A module. Sequence alignment indicates that an LDL-A module in LRP2 (LDL-A22) from both humans (16, 21) and rats (31) contains nine amino acids between the second and the third cysteines, exactly like that in Tva (Fig. 4). Thus, we predict that this module does not contain the signature antiparallel β-sheet and may adopt a three-dimensional conformation similar to that of the Tva module.

As discussed above, the N terminus of the Tva module does not contain the signature antiparallel β-sheet, suggesting a conformation of Tva more flexible than those of other LDL-A modules. To test this, backbone dynamics of the Tva LDL-A module and LRP CR8 were examined by measuring their ^{15}N longitudinal relaxation times (T_1), ^{15}N transverse relaxation times (T_2), and ^{1}H-^{15}N NOEs. These relaxation parameters were then used to perform a model-free analysis of internal motions using the program TENSOR 2 (8). Presented in Fig. 5 are squares of the generalized order parameters (S^2) for the Tva module (A) and for LRP CR8 (B), which describe the amplitude of the internal motions on the nanosecond-picosecond time scale. A higher S^2 value indicates more-restricted motion in a molecular reference frame, while a lower S^2 value indicates a more isotropic internal motion. In the Tva module (A), there is a large decrease in order for residues 23, 24, 25, 27, and 28, which corresponds to the region between the second (residue 18) and the third cysteines (residue 28). Therefore, consistent with our prediction, this region exhibits faster motion in backbone dynamics than the rest of the Tva module and the entire module of LRP CR8. In addition, as discussed above, only a few cross-peaks could be identified in the three-dimensional NOESY spectra at 298°K for the Tva LDL-A module. In contrast, many well-defined cross-peaks could be easily identified in similar experiments for CR3 and CR8 (6, 18), consistent with the notion that the N termini of both CR3 and CR8 are more rigid than that of Tva. The structural flexibility of the N terminus of the Tva module may help to optimize receptor-ligand interaction upon EnvA binding.

Implications in viral entry. Up to now, much of the knowledge of Tva as the viral receptor for ASLV-A entry has been derived from mutational analysis. Several residues within the Tva LDL-A module critical for viral receptor function have been identified; these include L34, H38, D46, E47, W48, and G49 (27, 28, 39, 40). Mutations of these residues adversely affected the viral receptor function of Tva, as previously demonstrated. As discussed above, D46 and E47 are involved in calcium coordination, so it is unlikely that these residues play a direct role in ligand recognition. In contrast, since the other four residues (L34, H38, W48, and G49) were not predicted to be involved in calcium coordination, it was proposed that these residues were involved in ligand binding (28). Now, with the NMR solution structure of the Tva module available, we have mapped each of these four residues to the structure and examined their roles in protein folding and in mediating ASLV-A entry (Fig. 6).

It is clear from Fig. 6 that the side chains of W48 and H38 are solvent exposed, strongly suggesting that they are ligand contact residues. In contrast, the side chain of L34 is totally buried in the interior of the structure, forming a hydrophobic

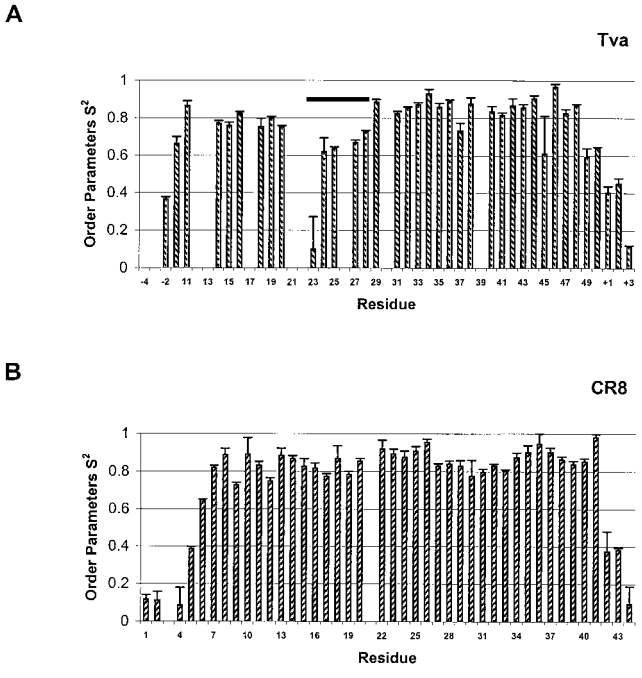

FIG. 5. Squares of the generalized order parameters by a model-free analysis of internal motions, S^2, of the Tva LDL-A module (A) and LRP CR8 (B). For the Tva LDL-A module, relaxation parameters were determined for 37 nonproline residues. The remaining four nonproline residues could not be determined due to spectrum overlapping or a weak signal. For LRP CR8, relaxation parameters were determined for 42 nonproline residues. Note that the residues at the N and C termini of the recombinant Tva module are derived from the vector and are designated − or +, respectively. The residues for CR8 are numbered as described by Huang et al. (18). Bar, residues between the second and the third cysteines of Tva with a low S^2 value.

Downloaded from http://jvi.asm.org/ on October 28, 2020 by guest

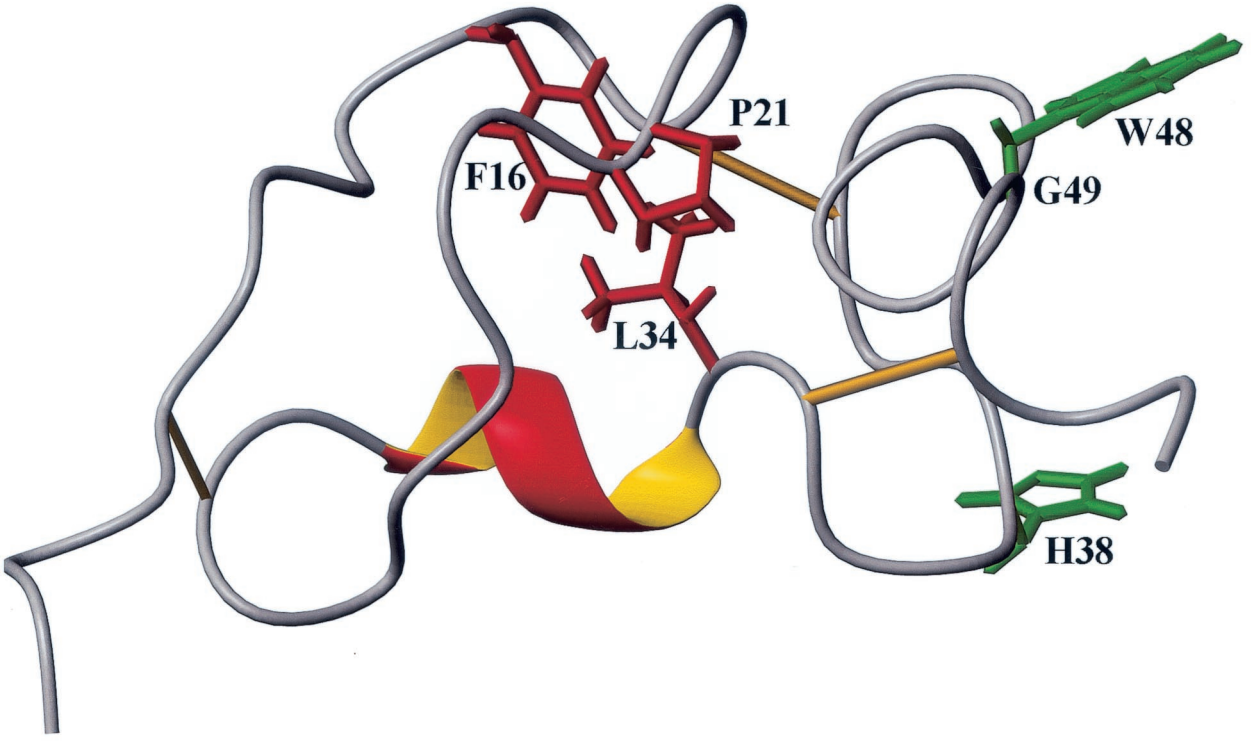

FIG. 6. Molecular model of Tva as the RSV-A receptor. The side chains of the putative ligand contact residues (green) are surface exposed, whereas the side chains of the residues involved in the formation of the hydrophobic core (red) are buried. In this model, it is proposed that the conformation of the more flexible N terminus of Tva is rigidified upon EnvA binding (induced fit).

core with F16 and P21, indicating that this residue plays a critical role in protein folding rather than in ligand recognition.

Previously we examined the Ca^{2+}-dependent folding properties of the wild-type (wt) Tva module and several mutants, including W48A and L34A mutants. It was found that folding of the L34A mutant protein was quite different from that of the wt Tva and W48A mutant protein, as demonstrated by high-pressure liquid chromatography, two-dimensional NMR (HSQC), and calorimetry (34). The structure of the Tva LDL-A module suggests that replacement of L34 with a small alanine may disrupt the hydrophobic core and lead to incorrect protein folding. However, the folding of the W48A mutant protein was similar to that of the wt Tva module, though minor differences were observed. It is likely that the replacement of tryptophan, an aromatic residue, with a small alanine can slightly alter the overall conformation of Tva due to changes in hydrophobicity and size. Nevertheless, together with previous mutational analysis, the structure of the Tva LDL-A module strongly suggests that the W48 is an important ligand (EnvA) contact residue.

The role of H38 in the viral receptor function of Tva was first identified by a gain-of-function approach (28). It was found that conversion of the human LDL-A4 module into a functional receptor for ASLV-A infection was dependent on the replacement of D23 with the corresponding residue of Tva (H38). Furthermore, replacement of H38 with an aspartate in Tva adversely affected viral receptor function. Although the carbonyl oxygen of H38 is involved in calcium coordination, we believe that this substitution in Tva (H to D) should not impair calcium binding or affect the overall structure of Tva. Sequence alignment indicates that the residues corresponding to H38 of Tva are not conserved among LDL-A modules (Fig. 4). Thus, the structure of the LDL-A module of Tva strongly suggests that H38, a basic residue of Tva, is an important viral interaction determinant. It is interesting that the X-ray crystal structure of the CD4-gp120 complex shows that F43 (an aromatic residue) of CD4 fits deep into a pocket within gp120 of human immunodeficiency virus (HIV) and makes multiple contacts with the hydrophobic residues of gp120. In addition, R59 (a basic residue) of CD4 interacts with multiple residues on gp120 (22). Perhaps both Tva and CD4 use residues with similar properties (W48 and H38 for Tva and F43 and R59 for CD4, respectively) in interacting with their cognate viral glycoproteins. This similarity suggests a possible common mechanism of ligand binding and receptor-triggered conformational changes on the viral glycoproteins among different retroviruses. W48 and H38 of Tva may be crucial for both EnvA binding and postbinding steps in ASLV-A entry. It is well established that entry of HIV depends on interactions of gp120 with both CD4 and chemokine receptors (7). If the role of Tva in ASLV-A entry is similar to that of CD4 in HIV infection, we would expect that an additional factor(s) may also be required. Interestingly, it was recently reported that low pH plays a critical role in ASLV-A entry (23). It is tempting to speculate that in ASLV-A infection low pH plays a role similar to that of chemokine receptors in HIV entry.

We previously observed the critical role of the N terminus (from the first to the third cysteine) of Tva in viral receptor function (27, 28). Recently we showed that conversion of the human LDL-A4 and LDL-A5 to a fully functional receptor of

Downloaded from http://jvi.asm.org/ on October 28, 2020 by guest

ASLV-A required the replacement of the N termini of these modules with the corresponding region from Tva (D. Marble, K. Rihani, F. Shaikh, and L. Rong, submitted for publication). These results further demonstrated the critical role of the amino terminus of the LDL-A module of Tva in ASLV-A infection, either structurally, functionally, or both. The NMR solution structure of the viral interaction domain of Tva reported here shows that the N terminus of this LDL-A module is folded differently from that of human LDL-A5, and likely that of human LDL-A4 as well. Therefore, the conformation of the N-terminal region may be crucial for the optimal viral receptor function of Tva. The flexible N terminus of Tva may adopt a more rigid conformation upon EnvA binding (induced fit) for optimal ligand binding and receptor triggering. In addition, sequence divergence of Tva in the region from the second to the third cysteine between quail and chicken (Fig. 4) may dictate subtle structure differences in this region and explain altered receptor specificity by ASLV-A variants (17).

Our current model is that W48 and H38 are directly involved in EnvA recognition. However, in contrast to our previous hypothesis, it is very unlikely that L34 directly contributes to ligand binding since it is part of the hydrophobic core (Fig. 6). Also, we believe that G49 is required to allow correct alignment of the adjacent tryptophan residue (W48), as we previously suggested. In addition, the flexible N-terminal structure of the module may change its conformation upon EnvA binding to promote high-affinity binding between Tva and EnvA. However, this awaits further structural analysis of Tva-EnvA complexes.

ACKNOWLEDGMENTS

Q.-Y.W. and W.H. contributed equally to this work.

We thank Michael Caffrey, Xiubei Liao, Wesley Sundquist, and Di Xia for helpful discussions and suggestions and Xiao Wu for computer assistance during the course of this study. We thank Michael Caffrey for critical reading of the manuscript.

This work was partially supported by American Heart Association Midwest Affiliate Grant-In-Aid 9951134Z (L.R.) and National Institutes of Health grants CA092459 (L.R.) and GM54414 (P.G.W.G.). L.R. was a recipient of the Schweppe Foundation Career Development Award. Q.-Y.W. was a recipient of the American Heart Association Midwest Affiliate Predoctoral fellowship.

REFERENCES

1. **Balliet, J. W., J. Berson, C. M. D'Cruz, J. Huang, J. Crane, J. M. Gilbert, and P. Bates.** 1999. Production and characterization of a soluble, active form of Tva, the subgroup A avian sarcoma and leukosis virus receptor. J. Virol **73:**3054–3061.
2. **Bates, P., J. A. T. Young, and H. E. Varmus.** 1993. A receptor for subgroup A Rous sarcoma virus is related to the low density lipoprotein receptor. Cell **74:**1043–1051.
3. **Daly, N. L., M. J. Scanlon, J. T. Tjordjevic, P. A. Kroon, and R. Smith.** 1995. Three-dimensional structure of a cysteine-rich repeat from the low-density lipoprotein receptor. Proc. Natl. Acad. Sci. USA **92:**6334–6338.
4. **Daly, N. L., J. T. Djordjevic, P. A. Kroon, and R. Smith.** 1995. Three-dimensional structure of the second cysteine-rich repeat from the human low-density lipoprotein receptor. Biochemistry **34:**14474–14481.
5. **Damico, R. L., J. Crane, and P. Bates.** 1998. Receptor-triggered membrane association of a model retroviral glycoprotein. Proc. Natl. Acad. Sci. USA **95:**2580–2585.
6. **Dolmer, K., W. Huang, and P. G. Gettins.** 2000. NMR solution structure of complement-like repeat CR3 from the low density lipoprotein receptor-related protein. Evidence for specific binding to the receptor binding domain of human α_2-macroglobulin. J. Biol. Chem. **275:**3264–3269.
7. **Doms, R. W., and J. P. Moore.** 2000. HIV-1 membrane fusion: targets of opportunity. J. Cell Biol. **151:**F9–F14.
8. **Dosset, P., J. C. Hus, M. Blackledge, and D. Marion.** 2000. Efficient analysis of macromolecular rotational diffusion from heteronuclear relaxation data. J. Biomol. NMR **16:**23–28.
9. **Farrow, N. A., R. Muhandiram, A. U. Singer, S. M. Pascal, C. M. Kay, G. Gish, S. E. Shoelson, T. Pawson, J. D. Forman-Kay, and L. E. Kay.** 1994. Backbone dynamics of a free and phosphopeptide-complexed Src homology 2 domain studied by ^{15}N NMR relaxation. Biochemistry **33:**5984–6003.
10. **Fass, D., S. Blacklow, P. S. Kim, and J. M. Berger.** 1997. Molecular basis of familial hypercholesterolaemia from structure of LDL receptor module. Nature **388:**691–693.
11. **Gilbert, J. M., P. Bates, H. E. Varmus, and J. M. White.** 1994. The receptor for the subgroup A avian leukosis-sarcoma viruses binds to subgroup A but not to subgroup C envelope protein. J. Virol. **68:**5623–5628.
12. **Gilbert, J. M., L. D. Hernandez, J. W. Balliet, P. Bates, and J. M. White.** 1995. Receptor-induced conformational changes in the subgroup A avian leukosis and sarcoma virus envelope glycoprotein. J. Virol. **69:**7410–7415.
13. **Grzesiek, S., and A. Bax.** 1992. Improved 3D triple-resonance NMR techniques applied to a 31 kDa protein. J. Magn. Reson. **96:**432–440.
14. **Guntert, P., C. Mumenthaler, and K. Wuthrich.** 1997. Torsion angle dynamics for NMR structure calculation with the new program DYANA. J. Mol. Biol. **273:**283–298.
15. **Hernandez, L. D., R. J. Peters, S. E. Delos, J. A. T. Young, D. A. Agard, and J. M. White.** 1997. Activation of a retroviral membrane fusion protein: soluble receptor-induced liposome binding of the ALSV envelope glycoprotein. J. Cell Biol. **139:**1455–1464.
16. **Herz, J., U. Hamann, S. Rogne, O. Myklebost, H. Gausepohl, and K. K. Stanley.** 1988. Surface location and high affinity for calcium of a 500-kd liver membrane protein closely related to the LDL-receptor suggest a physiological role as lipoprotein receptor. EMBO J. **7:**4119–4127.
17. **Holmen, S. L., D. C. Melder, and M. J. Federspiel.** 2001. Identification of key residues in subgroup A avian leukosis virus envelope determining receptor binding affinity and infectivity of cells expressing chicken or quail Tva receptor. J. Virol. **75:**726–737.
18. **Huang, W., K. Dolmer, and P. G. Gettins.** 1999. NMR solution structure of complement-like repeat CR8 from the low density lipoprotein receptor-related protein. J. Biol. Chem. **274:**14130–14136.
19. **Kay, L. E., G. Y. Xu, A. U. Singer, D. R. Muhandiram, and J. D. Formankay.** 1993. A gradient-enhanced HCCH-TOCSY experiment for recording side-chain ^{1}H and ^{13}C correlations in H_2O samples of proteins. J. Magn. Reson. Ser. B **101:**333–337.
20. **Koradi, R., M. Billeter, and K. Wuthrich.** 1996. MOLMOL: a program for display and analysis of macromolecular structures. J. Mol. Graph. **14:**51–55.
21. **Krieger, M., and J. Herz.** 1994. Structures and functions of multiligand lipoprotein receptors: macrophage scavenger receptors and LDL receptor-related protein (LRP). Annu. Rev. Biochem. **63:**601–637.
22. **Kwong, P. D., R. Wyatt, J. Robinson, R. W. Sweet, J. Sodroski, and W. A. Hendrickson.** 1998. Structure of an HIV gp120 envelope glycoprotein in complex with the CD4 receptor and a neutralizing human antibody. Nature **393:**648–659.
23. **Mothes, W., A. L. Boerger, S. Narayan, J. M. Cunningham, and J. A. T. Young.** 2000. Retroviral entry mediated by receptor priming and low pH triggering of an envelope glycoprotein. Cell **103:**679–689.
24. **Muhandiram, D. R., and L. E. Kay.** 1994. Gradient-enhanced triple-resonance three-dimensional NMR experiments with improved sensitivity. J. Magn. Reson. Ser B **103:**203–216.
25. **North, C. L., and S. C. Blacklow.** 2000. Solution structure of the sixth LDL-A module of the LDL receptor. Biochemistry **39:**2564–2571.
26. **Rong, L., and P. Bates.** 1995. Analysis of the subgroup A avian sarcoma and leukosis virus receptor: the 40-residue, cysteine-rich, low-density lipoprotein receptor repeat motif of Tva is sufficient to mediate viral entry. J. Virol. **69:**4847–4853.
27. **Rong, L., K. Gendron, B. Strohl, R. Shenoy, R. J. Wool-Lewis, and P. Bates.** 1998. Characterization of determinants for envelope binding and infection in Tva, the subgroup A avian sarcoma and leukosis virus receptor. J. Virol. **72:**4552–4559.
28. **Rong, L., K. Gendron, and P. Bates.** 1998. Conversion of a human low-density lipoprotein receptor ligand-binding repeat to a virus receptor: identification of residues important for ligand specificity. Proc. Natl. Acad. Sci. USA **95:**8467–8472.
29. **Rong, L., A. Edinger, and P. Bates.** 1997. Role of basic residues in the subgroup-determining region of the subgroup A avian sarcoma and leukosis virus envelope in receptor binding and infection. J. Virol. **71:**3458–3465.
30. **Rost, B.** 1996. PHD: predicting one-dimensional protein structure by profile-based neural networks. Methods Enzymol. **266:**525–539.
31. **Saito, A., S. Pietromonaco, A. K. Loo, and M. G. Farquhar.** 1994. Complete cloning and sequencing of rat gp330/"megalin"; a distinctive member of the low density lipoprotein receptor gene family. Proc. Natl. Acad. Sci. USA **91:**9725–9729.
32. **Talluri, S., and G. Wagner.** 1996. An optimized 3DNOESY-HSQC. J. Magn. Reson. Ser. B **112:**200–205.
33. **Vuister, G. W., and A. Bax.** 1993. Quantitative J correlation: a new approach for measuring homonuclear three-bond J ($H^{N}H^{\alpha}$) coupling constants in ^{15}N-enriched proteins. J. Am. Chem. Soc. **115:**7772–7777.

Downloaded from http://jvi.asm.org/ on October 28, 2020 by guest

34. **Wang, Q. Y., K. Dolmer, W. Huang, P. G. Gettins, and L. Rong.** 2001. Role of calcium in protein folding and function of Tva, the receptor of subgroup A avian sarcoma and leukosis virus. J. Virol **75:**2051–2058.
35. **Wishart, D. S., and B. D. Sykes.** 1994. Chemical shifts as a tool for structure determination. Methods Enzymol. **239:**363–392.
36. **Wittekind, M., and L. Mueller.** 1993. HNCACB, a high-sensitivity 3D NMR experiment to correlate amide-proton and nitrogen resonances with the alpha- and beta-carbon resonances in proteins. J. Magn. Reson. **B108:**94–98.
37. **Wuthrich, K.** 1986. NMR of proteins and nucleic acids. John Wiley & Sons, New York, N.Y.
38. **Zhang, O., L. E. Kay, J. P. Olivier, and J. D. Forman-Kay.** 1994. Backbone ^{1}H and ^{15}N resonance assignments of the N-terminal SH3 domain of drk in folded and unfolded states using enhanced-sensitivity pulsed field gradient NMR techniques. J. Biomol. NMR **4:**845–858.
39. **Zingler, K., C. Belanger, R. Peters, D. Agard, and J. A. T. Young.** 1995. Identification and characterization of the viral interaction determinants of the subgroup A avian leukosis virus receptor. J. Virol. **69:**4261–4266.
40. **Zingler, K., and J. A. T. Young.** 1996. Residue Trp-48 of Tva is critical for viral entry but not for high-affinity binding to the SU glycoprotein of subgroup A avian leukosis and sarcoma viruses. J. Virol. **70:**7510–7516.

Downloaded from http://jvi.asm.org/ on October 28, 2020 by guest